Fuel 182 (2016) 467–479

Contents lists available at ScienceDirect

Fuel

journal homepage: www.elsevier.com/locate/fuel

Full Length Article

Methodology for the experimental measurement of vapor–liquid equilibrium distillation curves using a modified ASTM D86 setup

Alison M. Ferris, David A. Rothamer *

Department of Mechanical Engineering and DOE Great Lakes Bioenergy Research Center, University of Wisconsin-Madison, 1500 Engineering Dr., Madison, WI 53706, USA

HIGHLIGHTS

- A method for obtaining experimental equilibrium distillation curves is proposed.
- The method utilizes time-resolved measurements of liquid and vapor temperature.
- A derivative based method is used to determine a fuel's true initial boiling point.
- Dynamic holdup is found to correlate with volatility and condenser bath temperature.

ARTICLE INFO

Article history:
Received 3 March 2016
Received in revised form 16 May 2016
Accepted 20 May 2016
Available online 8 June 2016

Keywords:
ASTM D86
Distillation curve
Dynamic holdup
Vapor–liquid equilibrium
Experimental equilibrium distillation curve
EEDC

ABSTRACT

A method has been developed to determine experimental equilibrium distillation curves using a modified ASTM D86 distillation apparatus.The method determines accurate equilibrium initial boiling points and accounts for the dynamic holdup inherent in distillation curves measured in accordance with the ASTM D86 standard.In this work, the ASTM D86 distillation setup has been modified to simultaneously measure liquid and vapor temperature using two resistance temperature detectors (RTDs) and a data acquisition system has been employed to record temperature data at one-second time intervals for the duration of each distillation.Additionally, the time for each volume recovery point is recorded.The method presented here uses the time-resolved liquid temperature data to identify the true initial boiling point (IBP) of four fuel mixtures of known composition; the IBPs are within 2 °C of the calculated equilibrium values.The time-resolved volume recovery information and the identified initial boiling point time are used to construct a volume evaporated versus time curve.The measured temperatures determined at the corresponding volume evaporated increments provide an experimental equilibrium distillation curve (EEDC). The EEDCs for the four fuel mixtures of known composition match the calculated equilibrium curves within a few degrees Celsius; a maximum mean absolute error of 2.2 ± 1.4 °C was observed.The dynamic holdup (volume difference between volume evaporated and volume recovered) associated with a distillation is found to correlate with the initial boiling point of the fuel being distilled and the temperature of the condenser bath used in the experiment.The method was also applied to measure EEDCs for a gasoline fuel and a diesel fuel, where the compositions were unknown, to investigate the differences between the EEDCs and the ASTM D86 distillation curves.The results highlight the large errors incurred when using ASTM D86 results to approximate equilibrium distillation curves.

1. Introduction

Petroleum-derived gasoline is a complex blend of hundreds of hydrocarbons, primarily n-alkanes, iso-alkanes, naphthenes, olefins, aromatics, and oxygenates [1]. While the exact composition of a commercial gasoline blend is not regulated or defined, the volatility requirements for petroleum-derived gasoline in the United States are defined in the American Society for Testing and Materials (ASTM) D4814 Standard Specification for Automotive Spark-Ignition Engine Fuel [2]. Volatility is an indication of a fuel's tendency to vaporize; a very volatile fuel can easily transition from the liquid phase to the vapor phase under standard atmospheric conditions. The ASTM D4814 standard outlines gasoline volatility property requirements and their limits in different regions of the United States at different times of the year.

The production of fuel components made from bio-derived feedstocks, specifically sugars, starches, vegetable oils, and

* Corresponding author.
E-mail address: rothamer@wisc.edu (D.A. Rothamer).

http://dx.doi.org/10.1016/j.fuel.2016.05.099
0016-2361/

lignocellulosic biomass [3] offers the opportunity to reduce the CO_2 emissions associated with liquid fuels. If next-generation biofuels are to serve as drop-in replacements for conventional gasoline, they must meet appropriate fit-for-purpose volatility requirements. The volatility requirements described in ASTM D4814 are governed by a fuel's distillation curve, Reid vapor pressure (RVP), temperature for a vapor–liquid ratio of 20 ($T_{V/L=20}$), and driveability index (DI). A fuel's distillation curve, RVP, and $T_{V/L=20}$ are directly measurable quantities, while the drivability index is a correlation based on the distillation curve.

ASTM D86 is the standard test method used to experimentally measure the batch distillation curve of a petroleum-derived fuel at atmospheric pressure [4]. A distillation curve obtained using the ASTM D86 method is commonly known as a D86 distillation curve. Despite the slight procedural nuances associated with the distillation of a particular fuel type, the overall ASTM D86 apparatus setup and procedure remain the same. A 100-mL sample of fuel is boiled in a 100-mL or 125-mL distillation flask at atmospheric pressure. Heat is applied to the bottom of the flask using an electric heater or gas Bunsen burner. The top of the flask is sealed using a thermometer centering plug, which accommodates a mercury-in-glass or equivalent thermometer and prevents vapor leakage. The thermometer is positioned to measure the temperature of the fuel vapor as it rises and exits the neck of the distillation flask. The flask sidearm is tightly fitted into the distillation apparatus condenser tube, which passes through an insulated condensing bath.

A distillation measurement begins when heat is first applied to the bottom of the distillation flask. As the distillate is heated and begins to boil, fuel vapor rises out of the distillation flask and travels through the condensing bath. The condensate is collected in a receiving cylinder. The D86-specified initial boiling point (IBP) of a fuel is taken to be the temperature of the fuel vapor, measured by the thermometer in the flask neck, when the first drop of condensate falls into the receiving cylinder. As the distillation progresses and condensate collects, the vapor temperature is recorded at every 5-mL (or 5 vol%) interval, as measured by the graduated cylinder.

The average rate of distillation should be kept constant at 4–5 mL/min from the time that 5 mL of fuel has condensed to the point that 5 mL of fuel remains in the distillation flask. When the liquid volume remaining in the flask is approximately 5 mL, the heat is significantly increased in an effort to vaporize the least volatile components in the flask. The maximum vapor temperature attained is taken to be the end point (EP) of the distillation.

A fuel's distillation curve is of particular interest because its characteristics can be related to various operational parameters, including engine start-up, driveability, vapor lock, fuel system icing, fuel economy, and even emissions [5–7]. Due to the importance of a distillation curve's shape and its implications for engine performance and emissions, distillation curves have been identified as a valuable metric for measuring the overall volatility and driveability of a fuel, and have served as a basis for the modeling and development of gasoline-like fuel mixtures with desirable volatility properties.

Unfortunately, discrepancies have been observed between modeled distillation curve results, derived from thermodynamic relations describing vapor–liquid equilibrium, and the results measured according to the ASTM D86 standard. The vaporization process of a fuel is characterized by vapor–liquid equilibrium, but it is widely acknowledged that this equilibrium process is not accurately captured by an ASTM D86 distillation curve, due to the location of the D86 temperature measurement and the measurement of volume recovered instead of volume evaporated [8–10]. These discrepancies make it difficult to predict using equilibrium calculations alone, without experimental testing, whether or not a given fuel blend will meet published volatility regulations. Recent work has therefore focused on both measuring and calculating the vapor–liquid equilibrium curves of gasoline-like fuels.

Bruno devised an advanced distillation apparatus for the purpose of both accurately measuring thermodynamic states and monitoring vapor composition throughout the batch distillation process [11]. The apparatus designed to accomplish this task is a variation on the original ASTM D86 distillation apparatus. In addition to an aluminum heating jacket and custom-made receiver, the apparatus includes two J-type thermocouples – one to measure the vapor temperature in the flask neck, as described in ASTM D86, and one to measure the liquid temperature in the distillation flask, thought to approximate a true thermodynamic state [10]. Measurement of the liquid temperature throughout the distillation is not a new approach; Greenfield et al. used liquid temperature measurements to validate their D86 distillation curve prediction model [8].

While measuring the liquid temperature of a fuel over the course of a distillation yields a measurement that is more representative of what is being modeled in a vapor–liquid equilibrium process, moving the temperature probe alone does not completely fix the discrepancy seen between measured and modeled distillation curves. This is illustrated in Fig. 1, which compares the liquid temperature curve, the ASTM D86 vapor temperature curve, and the calculated equilibrium distillation curve for a 50/50 n-decane/n-tetradecane mixture. The liquid temperature curve in Fig. 1 is labeled as D86 liquid; this signifies that this is the liquid temperature measured at the same 5% recovery intervals used in the ASTM D86 standard. Despite the significant improvement over the D86 vapor curve seen for the liquid temperature measurement, there is clear disagreement between the liquid distillation curve and the calculated equilibrium curve over the entire distillation.

Bruno also modified the D86 procedure to use the liquid temperature measurement to obtain a more accurate initial boiling point temperature. Instead of taking the initial boiling point to be the temperature as the first drop of condensate enters the graduated receiving cylinder, Bruno identified the initial boiling point as the temperature at which saturated vapor begins to rise out of the distillation flask [10].

Thermodynamically, the time of vapor rise is a logical indicator of initial boiling, as it corresponds to the beginning of the phase transformation from liquid to vapor. As such, this temperature

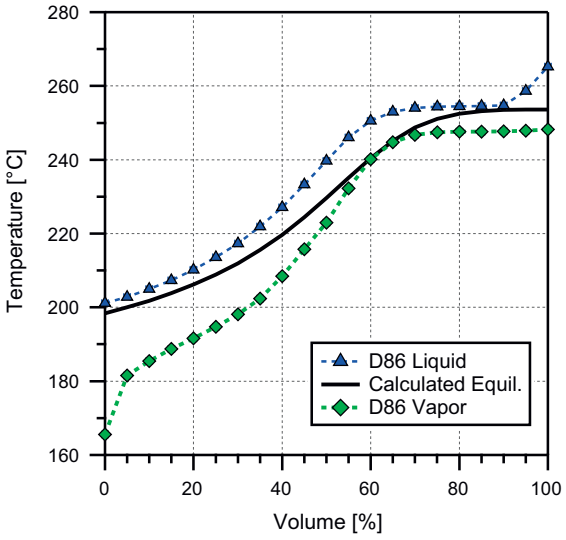

Fig. 1. ASTM D86 vapor temperature distillation curve, liquid temperature distillation curve, and calculated equilibrium distillation curve for a 50/50 (% mole fraction) n-decane/n-tetradecane mixture. Error bars are included, but are often smaller than the marker size.

point corresponds to the 0 vol% (0% evaporated) point of a calculated equilibrium distillation curve. In contrast, the 0 vol% fraction point used in D86 distillations corresponds to the first drop of condensate entering the receiving cylinder, which does not occur until later in the distillation process; the vapor from the flask bulb must first travel up the neck of the distillation flask, down the sidearm, and into the condenser tube where it will condense before dripping into the receiver. The percent volume associated with experimental liquid distillation curve temperature measurements corresponds to a percent volume collected post-condensation in the receiver, not a percent volume evaporated. This difference between the percent volume evaporated and the percent volume recovered at a given point in a distillation is termed dynamic holdup.

In order to develop a test method to more accurately measure the equilibrium distillation curve of a fuel, it is important to address the two factors causing the discrepancy between standard ASTM D86 distillation curves and modeled vapor–liquid equilibrium curves: measurement of the vapor temperature instead of the liquid temperature and lag in mass transfer through the D86 distillation apparatus (dynamic holdup).

In this work, the traditional ASTM D86 distillation apparatus has been modified to allow for time-resolved liquid temperature measurements and a method has been developed to correct for the dynamic holdup inherent in experimental distillation curves. Four fuel mixtures of known composition have been used to validate the method. Finally, the method has been used to investigate the equilibrium and D86 distillation curves for two petroleum distillate fuels of unknown composition.

2. Materials and methods

2.1. Fuel mixtures of interest

Four fuel mixtures were investigated in this work: (1) a 50/50 (mol/mol) mixture of n-decane/n-tetradecane; (2) a 50/50 mixture of n-heptane/n-pentane; (3) a mixture of iso-octane, n-heptane, and ethanol; and (4) a mixture of 1-butene, 1-hexene, methyl pentanoate, and ethyl levulinate. For each mixture, the individual components were poured into a 1-l container, the mass of which was recorded after the addition of each component. Creating the mixtures on a mass-basis allowed for easy conversion to mole fraction. The mole fraction uncertainty due to mixing based on mass was $\leqslant$0.001. The mixture compositions and the component purities are listed in Table 1. The listed purities are those reported by the fuel component suppliers (Sigma–Aldrich/Alfa Aesar).

2.2. Distillation apparatus, modifications, and data acquisition

A commercially available, manual distillation apparatus (Koehler model K45200) was used to perform the distillations. The apparatus meets all ASTM D86 specifications pertaining to dimensions and suitable component materials. The apparatus was outfitted with a 1000-W electric heater with variable control. The heater was mounted on an adjustable elevator plate, the height of which can be changed via a rack and pinion mechanism.

Table 1
Composition and component purity of investigated fuel mixtures.

	Component name	Mole fraction	Component purity (%)
Mixture 1	n-Decane	0.500	$\geqslant$99.0
	n-Tetradecane	0.500	$\geqslant$99.0
Mixture 2	n-Heptane	0.500	$\geqslant$99.0
	n-Pentane	0.500	$\geqslant$99.6
Mixture 3	Iso-octane	0.651	$\geqslant$99.5
	n-Heptane	0.136	$\geqslant$99.0
	Ethanol	0.212	96.2
Mixture 4	1-Butene	0.121	$\geqslant$99.0
	1-Hexene	0.471	$\geqslant$96.5
	Methyl pentanoate	0.335	$\geqslant$99.0
	Ethyl levulinate	0.073	$\geqslant$98.0

The experimental setup used in this work includes many standard ASTM D86 distillation apparatus components. A 125-mL, borosilicate glass, sidearm distillation flask was used for each distillation. A 100-mL graduated cylinder with 1.0-mL graduation intervals collected the condensate as it exited the condenser tube. To reduce evaporative losses of the distillate from the receiving cylinder, a plastic plate and a Kimwipe were used to cover the receiving cylinder during distillations. A hole in the wipe allows it to fit snugly around the condenser tube exit and a small plastic plate with a similar hole at its center rests on top of the wipe to hold it in place. Before the onset of initial boiling, the graduated cylinder was centered under the condenser tube exit to allow the first drop of condensate to fall freely to the bottom of the cylinder. After the first drop of condensate, the graduated cylinder was swiftly moved and brought into contact with the end of the condenser tube, which exits the distillation apparatus at a downward angle and is curved slightly backward to facilitate contact. Bringing the graduated cylinder into contact with the condenser tube exit eliminates splashing and allows for smooth condensate collection. Chemically inert marble boiling chips ($CaCO_3$) were used in each distillation to promote boiling and minimize superheating of the distillate liquid. Atmospheric pressure at the time of each distillation was recorded using a Bourdon tube aneroid barometer with 0.05 psi resolution.

Three modifications were made to the standard distillation apparatus setup to allow for more accurate temperature measurement and streamlined data collection. First, high-accuracy platinum resistance temperature detectors (RTDs) were used instead of ASTM D86-specified mercury thermometers. Each RTD contains a precision 100-Ohm Class A DIN platinum element (temperature coefficient of resistance, $\alpha = 0.00384\ ^\circ C^{-1}$) and has a temperature range of -200 to 500 °C. The temperature uncertainty associated with the RTD measurement ranges from 0.20 to 0.55 °C over the temperature range of interest for gasoline distillations ($\sim$25 to 200 °C). In comparison, the experimental accuracy of an ASTM-adherent distillation thermometer is $\pm$1.0 °C over the range of interest.

An RTD probe, by design, will not exhibit the same emergent stem error observed in a mercury-in-glass thermometer. However, ASTM D86 requires that reported temperature measurements emulate those of a mercury-in-glass thermometer. The ASTM D86 standard therefore provides an equation to adjust the electronic sensor reading so that it emulates that of a thermometer (emergent stem error emulation) [4]. It was found that the difference in temperature lag observed between a mercury thermometer and the RTD probe/electronic data collection system was statistically insignificant. Therefore, by substituting an RTD probe for a thermometer and applying emergent stem error emulation to the RTD measurement, a true ASTM D86 distillation curve can be produced. All distillation curves reported as D86 vapor distillation curves in this work incorporate the emergent stem error emulation. All other distillation curves were recorded using the true RTD temperature measurements.

As a second modification to the original distillation setup, a Teflon adapter was made to simultaneously accommodate two temperature probe locations: one in the flask bulb and one in the flask neck (see Fig. 2). The RTD in the flask bulb measures the distillate liquid temperature. The tip of this RTD is located 15 mm above the bottom of the flask – just high enough to avoid interference with the boiling chips used in each distillation. The RTD in the flask neck measures the vapor temperature of the distillate at the

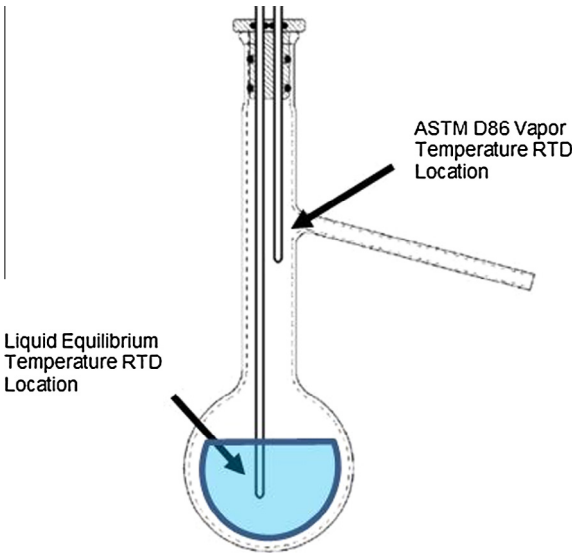

Fig. 2. ASTM D86 distillation flask with RTD adapter and vapor/liquid RTDs.

location specified in ASTM D86, i.e., 14 mm below "the highest point on the bottom of the inner wall of the [flask's] vapor tube" [4]. Each RTD is offset from the central axis of the adapter by 3.8 mm.

A National Instruments (NI) cDAQ-9174 chassis and NI 9217 data acquisition module were used in conjunction with a custom-developed LabVIEW VI to simultaneously acquire the RTD vapor and liquid temperature measurements. The measurements were sampled and recorded at 1 Hz, from the first application of heat to the end point of each distillation. Temperature measurements were also recorded at the distillation IBP (first drop of condensate), at every 5-mL volume interval, and at the distillation EP (highest vapor temperature) in accordance with the ASTM D86 test procedure.

All reported temperatures have been corrected for barometric pressure through application of the Sydney Young equation and are reported at standard atmospheric pressure (101.3 kPa). Use of the Sydney Young correction and its application to distillation curves are discussed next in Section 3.1.

3. Theory/calculations

3.1. Application of the Sydney Young equation

To provide an equivalent basis for comparison between distillation curves measured in different locations, the final reported temperature measurements for a D86 distillation curve are corrected for barometric pressure through application of the Sydney Young equation [4].

$$C_{std} = A\left[\frac{P_{std} - P_{obs}}{P_{std}}\right]T_{obs} \quad (1)$$

In Eq. (1), A is an empirical unitless coefficient of proportionality ($A = 0.0912$), T_{obs} is the temperature, measured on an absolute temperature scale, observed at local ambient pressure, P_{obs} is the local barometric pressure observed at the time of the distillation, P_{std} is the standard atmospheric pressure at sea level (101.3 kPa), and C_{std} is the correction that must be added to the observed temperature to obtain an equivalent temperature measurement at standard atmospheric pressure.

The fidelity and application of the Sydney Young shift to distillation curves have been explored by Ott et al. [12], who found that as atmospheric pressure decreases (or elevation increases), the Sydney Young correction becomes increasingly inaccurate. These findings agree with the recommendation set forth by the Organization for Economic Co-operation and Development (OECD), which suggests that the Sydney Young equation only be used to compensate for atmospheric pressure deviations of less than 5 kPa from standard atmospheric pressure [13].

Typical ambient pressure measured in the laboratory at the time of the distillation measurements was found to be approximately 98 kPa – well within the suggested pressure range for application of the Sydney Young equation. All temperature data points presented in this paper are reported at standard atmospheric pressure, i.e., the Sydney Young equation has been used to correct the data.

3.2. Calculation of equilibrium distillation curves

The methodology used to calculate the vapor–liquid equilibrium curves and estimate the IBP of each fuel is described in detail in [14]. It incorporates a thermodynamic model of the batch distillation process where the liquid phase is treated as non-ideal but the vapor phase is treated as an ideal gas. The evolution of the component mole fractions during the distillation are described by the Rayleigh equation [15], which provides a set of N (where N is the number of component species) ordinary differential equations that can be integrated to give the mole fractions as a function of the moles of distillate remaining. The mole fractions from the solution of the Rayleigh equation are used to iteratively solve for the mixture temperature at each distillation step. The volume of distillate throughout the distillation is calculated based on the moles of liquid distillate remaining and the mole fractions at each solution step using the individual component densities, assuming ideal mixing behavior. The resulting temperature versus volume distilled is interpolated to 5 vol%-distilled increments to match the measurement interval used for the D86 distillations.

Group contribution methods are used to calculate the thermodynamic properties. The UNIFAC group contribution method [16] is used to determine activity coefficients needed to calculate the equilibrium ratios and total vapor pressure for the mixture. The UNIFAC method accounts for non-ideal behavior due to interactions between components in the liquid. Individual component vapor pressures are calculated using the Antoine equation with coefficients obtained from Yaws' Handbook of Antoine coefficients [17]. The GCVOL-OL-60 group contribution method is used to calculate the liquid density of each mixture component [18].

The model approximates the vapor phase as an ideal gas and the liquid as following ideal mixing behavior for the calculation of liquid mixture volume. The ideal gas approximation is accurate at atmospheric total pressure for non-polar or slightly polar molecules [19]. Error associated with the ideal liquid mixing approximation is anticipated to be smaller than errors associated with the vapor pressures calculated from the Antoine coefficients and the activity coefficients determined from UNIFAC. The UNIFAC activity coefficients are believed to be the largest source of error for the equilibrium distillation curve calculations. Based on analysis of the accuracy of UNIFAC for a wide range of compounds for VLE calculations, the temperature uncertainty for the equilibrium distillation curves is estimated to be ±1.25 K (±1 standard deviation) [20].

3.3. Experimental equilibrium distillation curve method

A methodology for determining experimental equilibrium distillation curves was developed to account for dynamic holdup and evaporative losses, and to identify the true initial boiling point of a fuel. To understand how this methodology is derived, a con-

ceptual model of the ASTM D86 distillation process was developed and is described here.

The first step in the distillation process involves heating the mixture until it begins to boil. As the true initial boiling point is approached, the concentration of fuel vapor in the flask increases. This is due to the increasing partial pressure of the highest volatility components and expansion of the gases above the liquid due to increasing temperature. Time-resolved images, taken at 1-s intervals with a scientific interline CCD camera (Princeton Instruments model RTE/CCD-1300-Y/DIF, with a Nikon 24–50 mm *f*/3.3–4.5 D Nikkor lens), showed that the transition from initial vaporization to full boiling near the initial boiling point is relatively rapid, occurring over approximately 30 s.

It is assumed that there is little to no mass flow out of the distillation flask sidearm and that no condensed liquid is present in the condenser tube up until the true initial boiling point. Once boiling starts, it is assumed that the distillation rate, i.e., volumetric rate of evaporation, quickly reaches a near steady-state value of 4–5 mL/min of liquid as specified in the D86 standard. During the time between the true initial boiling point and the D86 initial boiling point, there is a flow of vaporized fuel into the condenser, but no flow out of the condenser tube. Assuming a constant mass flow into the condenser and no outflow tells us from conservation of mass that

$$\frac{dM_c}{dt} = \dot{m}_{in} \tag{2}$$

where M_c is the mass of fuel in the condenser tube and $\dot{m}_{in}$ is the mass flowrate of vaporized fuel into the condenser tube. Therefore, fuel mass is accumulating in the condenser tube during the period from the true initial boiling point to the time at which the first drop of condensate falls into the receiving cylinder.

Some of this fuel mass is assumed to collect on the condenser tube wall as condensed liquid droplets. Mass accumulates on the wall until either the mass of some of the droplets is sufficient to overcome surface tension and the droplets begin to flow out of the tilted condenser tube, or the wall is completely wetted and flow begins. Once flow begins out of the condenser tube, it is assumed that the rate of mass inflow into the condenser and mass outflow into the receiving cylinder are equal and the stored mass in the condenser tube remains approximately constant. This approximation breaks down near the end boiling point and may not hold strictly true throughout the distillation. As such, this approximation may limit the accuracy of the current model. The validity of the constant mass storage assumption is discussed in more detail in Section 3.3.2.

The mass on the surface of the condenser tube walls is usually the source of the majority of mass contributing to the dynamic holdup. For a typical ASTM D86 distillation setup, the volume above the liquid in the flask plus the sidearm volume and volume of the condenser tube is approximately 100–150 cm^3. If fuel vapor of a typical hydrocarbon (e.g., n-heptane) was to fill this volume, it would account for approximately 0.5–1 mL of liquid dynamic holdup. Since dynamic holdup can be as high as 10 mL of liquid for certain mixtures, a large fraction of the dynamic holdup in these cases is stored as liquid on the walls of the condenser tube.

To determine the equilibrium distillation curve, which accounts for dynamic holdup, the true initial boiling point of the mixture must first be identified. Next, the temperature at which each proceeding 5% evaporation point occurs must be obtained, followed by identification of the distillation end point. Finally, the dynamic holdup can be determined. Each of these steps is described in the following sections, concluding with an analysis of the results.

3.3.1. IBP identification

The onset of boiling can be identified through visual confirmation of vapor rise, which is indicated by the movement of condensed vapor droplets convected with the saturated vapor expanding from the distillation flask bulb to the flask neck. However, vapor rise is not always easy to spot, as it depends upon condensation of some of the fuel vapor, which will not always occur, especially for very volatile fuel mixtures. Visual identification of vapor rise is also somewhat subjective, making it prone to inaccuracy. A more consistent, objective method for identifying the IBP of a mixture is presented here.

As discussed previously, the true IBP of a mixture occurs before the IBP identified using the ASTM D86 standard procedure (corresponding to the first drop of condensate in the receiver). Therefore, it is necessary to collect temperature data before the ASTM D86 IBP to allow experimental measurement of the true IBP. The modified ASTM D86 distillation setup outlined in Section 2.2 allows for time-resolved liquid and vapor temperature measurement before the ASTM D86 IBP.

A representative plot of the time-resolved temperature data collected for a single 50/50 n-decane/n-tetradecane distillation can be seen in Fig. 3. The continuous liquid and vapor temperatures are plotted as a function of time, from the first application of heat until all vapor was observed to have exited the flask. Because the vapor rise out of the flask bulb was readily apparent for this mixture, temperature data points were logged when the vapor front was first observed exiting the flask bulb and when it passed the tip of the vapor RTD located in the neck of the flask; these data points are superimposed on both the liquid and vapor temperature curves. The data points collected for a traditional D86 distillation (at the first drop of condensate and every 5 mL interval of condensed liquid thereafter) were recorded and are also superimposed on the time-resolved vapor temperature curve.

Vapor rise out of the flask bulb was seen to occur approximately 600 s into the distillation. This point corresponds to a drastic change in slope (large curvature) in the liquid temperature vs. time curve. After vapor rise is observed, the liquid temperature begins to plateau. Approximately 35 s later, the vapor front passes the tip of the RTD located in the flask neck, and shortly thereafter the vapor temperature measured by the RTD in the D86 location rises sharply.

In five distinct distillations of the same n-decane/n-tetradecane mixture, the point at which vapor begins to rise out of the flask

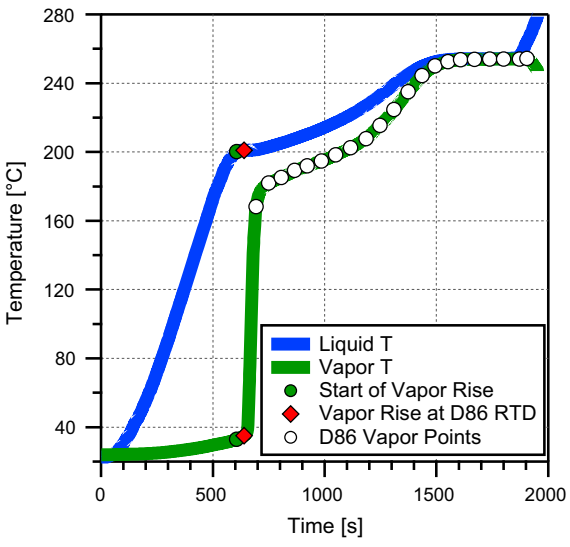

Fig. 3. Time-resolved vapor and liquid temperature with D86 distillation curve and vapor rise indicators (50/50 n-decane/n-tetradecane mixture).

bulb consistently lines up with a change in curvature in the time-resolved liquid temperature data. The calculated equilibrium IBP for a 50/50 n-decane/n-tetradecane mixture distilled at standard atmospheric pressure is 198.4 °C. As seen in Fig. 4, this point is reached when the slope of the liquid temperature curve begins to significantly decrease and plateau.

It appears that an extreme value of curvature does in fact approximate the point at which the mixture transitions from simply being heated, to boiling. The challenge is then to consistently and accurately identify this extreme curvature point in the time-resolved liquid temperature data, regardless of the sample being considered, in the presence of experimental noise.

Because a large negative curvature is seen to correspond to the IBP, the second derivative of the liquid temperature was calculated with respect to time for each of the four mixtures of interest and a minimum in this trace was sought near the IBP time. Because the D86 IBP time is recorded, the region of interest can be limited to a time period shortly before and after the D86 IBP time.

The procedure for identifying the true IBP is as follows. First a high-order polynomial curve fit was applied to the liquid temperature versus time data. The fit was first performed for a time range starting 180 s before the D86 IBP and extending to 240 s after the D86 IBP. A minimum in the 2nd derivative of the liquid temperature versus time was sought in a region starting 120 s before the D86 IBP up to the D86 IBP. This region was chosen because the D86 IBP always occurs after the true IBP. The time period of 120 s was chosen because typical D86 distillation rates are 5 mL/min, so as long as the amount of dynamic holdup is less than about 10 mL, the true IBP is expected fall in this time period.

Once the minimum is found, a high-order polynomial is fit again to the liquid temperature versus time data for the time period starting 120 s before the initially estimated true IBP time and stopping 120 s after. It is necessary to perform a second polynomial fit to the data, this time over a smaller timeframe, in order to more accurately detect the location of the 2nd derivative minimum. The local minimum in the curvature of the liquid temperature is then found again in the subset of time 60 s before and after the initially estimated true IBP time. The time of this local minimum is then considered to be the true IBP time, and the corresponding temperature, the true IBP temperature.

Fig. 5 shows the 2nd derivative of temperature versus time for the polynomial curve fit for one run of each of the four mixtures studied. The times corresponding to the initial boiling points from the calculated equilibrium distillation curves are also shown. From the plots in Fig. 5, it can be seen that each second derivative reaches a local minimum in the time frame of interest. Also, the time corresponding to the minimum closely matches the time at which the true initial boiling point of each mixture is thought to occur, based on the calculated equilibrium curve predictions. The maximum time difference between the occurrence of the calculated initial boiling point and the second derivative minimum is 18.6 s, observed for run 3 of Mixture 3 (iso-octane, n-heptane, and ethanol).

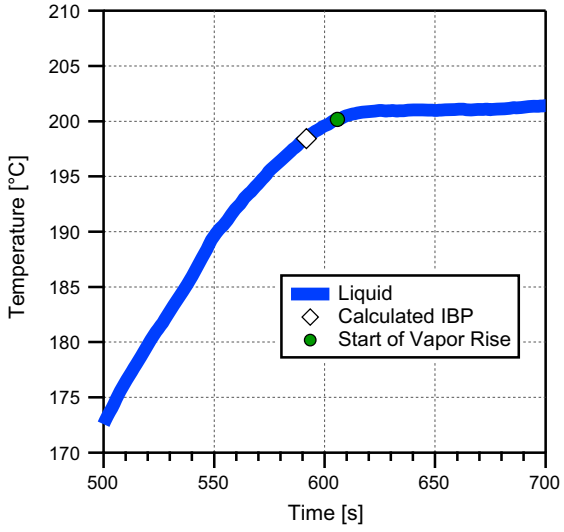

Fig. 4. Subset of time-resolved liquid temperature data showing location of calculated IBP and observed vapor rise out of flask bulb (50/50 n-decane/n-tetradecane mixture). Line thickness for liquid temperature indicates approximate temperature uncertainty.

This iterative process has proven to be robust for a wide range of distillation curves. However, visual verification of the 2nd derivative in the region of interest is also performed, as once in a great while, due to fluctuations in the liquid temperature data, two local minima are present in the region of interest. The true IBP always corresponds to the later of these two minima. When this is the case, the second minimum is manually selected. For the thirteen distillations presented in this paper, manual selection only occurred for one case: run 1 of Mixture 1.

The use of a high-order polynomial fit to determine the 2nd derivative minimum was motivated by the need to reduce noise. Directly numerically differentiating the liquid temperature data twice results in a noisy curve that makes it impossible to locate the 2nd derivative minimum. To fully resolve the frequency range of changes present, a relatively high-order polynomial is required. The determination of IBP time is relatively insensitive to the order of the polynomial used beyond a certain order (50th order). For the current work 90th order polynomials are utilized, but represent the high end of the order that should be used, since multiple data points are desired per polynomial coefficient.

An analysis of the agreement between the temperature corresponding to the location of the second derivative minimum and the calculated initial boiling point was carried out. Multiple distillation runs were performed for each mixture. The polynomial fitting method was used on each raw liquid temperature trace and the minimum of the second derivative with respect to time was determined as just described. The difference in temperature between the IBP identified using the second derivative approach and the calculated IBP, as well as, the difference in time between the location of the second derivative minimum and the calculated IBP for each distillation run, are reported in Table 2.

It can be seen in Table 2 that regardless of mixture composition, the minimum of the second derivative consistently identifies each mixture's IBP within 2.1 °C of the calculated IBP. The IBP is also consistently identified within 18.6 s of the calculated IBP time. It should be noted that although the results in this paper are compared to the calculated equilibrium reference curves, the calculated equilibrium curves themselves have uncertainties associated with them, as previously mentioned in Section 3.2. Therefore, the calculated equilibrium curves should not be viewed as an absolute reference, but instead, their uncertainty must also be considered.

3.3.2. Calculation of experimental equilibrium distillation curve (5–95 mL) and dynamic holdup volume

Once the location of the true initial boiling point has been identified using the minimum of the 2nd derivative, the remaining points of the distillation curve, exclusive of the end point, can be located by converting the measured volume recovered versus time into volume distilled (volume evaporated) versus time. In doing so, an experimental equilibrium distillation curve, unaffected by dynamic holdup, can be obtained.

The modified distillation apparatus used for this work allows the time and temperature at each 5-mL recovered volume increment (each D86 distillation curve point) to be recorded. The evap-

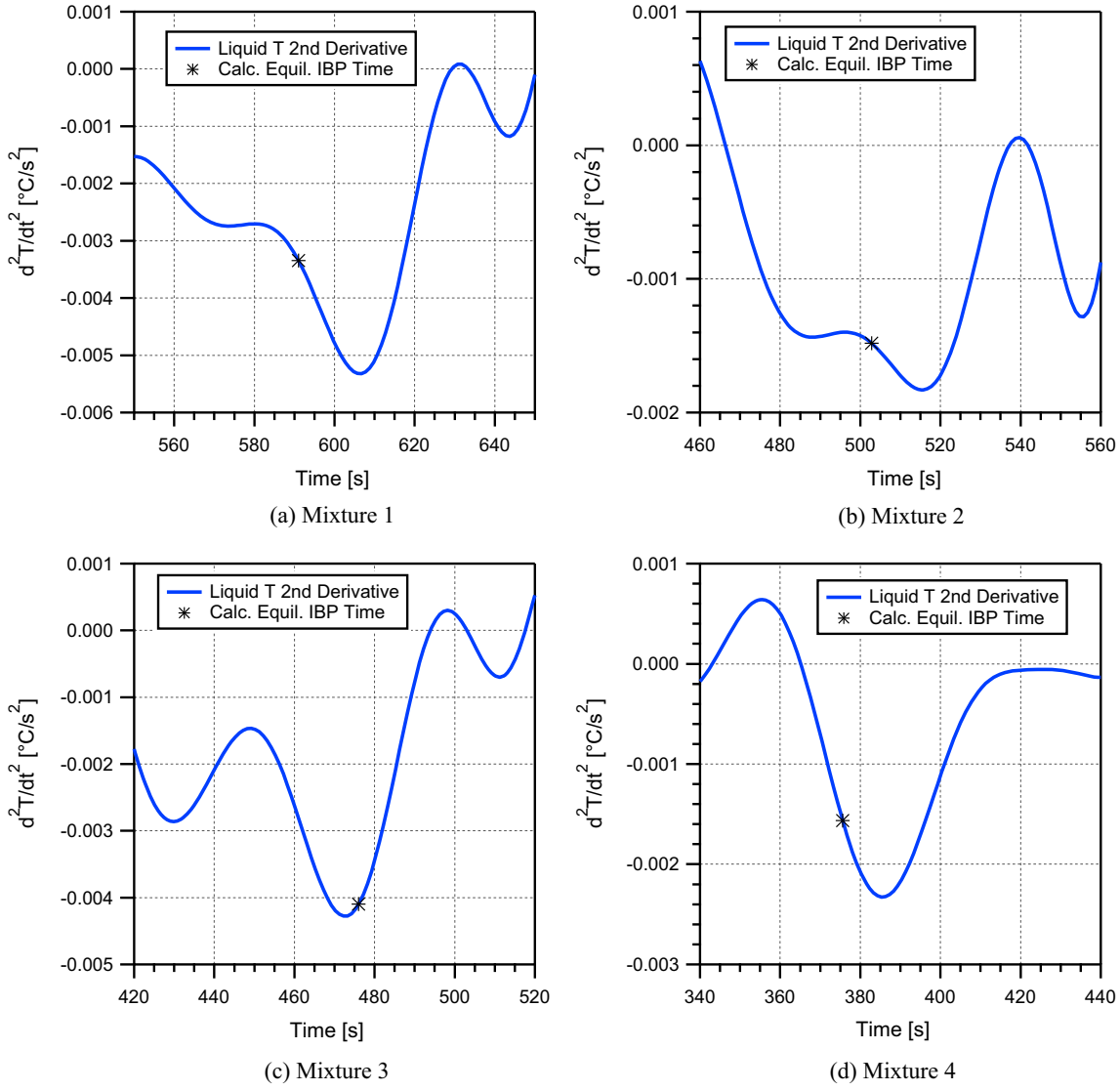

Fig. 5. Subset of liquid temperature second derivative with respect to time, focusing on initial boiling region, for representative distillations of the four mixtures of interest: (a) Mixture 1 (50/50 n-decane/n-tetradecane), (b) Mixture 2 (50/50 n-heptane/n-pentane), (c) Mixture 3 (iso-octane, n-heptane, and ethanol), and (d) Mixture 4 (1-butene, 1-hexene, methyl pentanoate, and ethyl levulinate). Asterisk denotes time of the calculated equilibrium IBP.

orated volume is directly related to the recovered volume at any given time by:

$$V_{evap}(t) = V_{rec}(t) + V_{loss} + V_{dh} \tag{3}$$

where V_{evap} is the current volume evaporated from the distillation flask, V_{rec} is the current volume recovered in the receiving cylinder, V_{dh} is the equivalent liquid volume dynamic holdup, and V_{loss} is the equivalent liquid volume of any vapor lost from the receiving cylinder or not condensed. The volume recovered in the experiments is measured versus time, so determination of the volume evaporated corresponding to an equilibrium distillation requires estimation of the sum of V_{dh} and V_{loss}.

After an initial transient period, the evaporation rate is assumed to be equal to the recovery rate. Therefore, the evaporated volume versus time curve can be determined from the recovered volume versus time curve according to Eq. (3). The losses are known by subtracting the total volume recovered from the initial volume. For the more volatile mixtures studied in this work, losses were ≈1–2 mL (1–2%). It is assumed that all of the losses occur around the time of the initial boiling point or shortly thereafter. To determine the dynamic holdup volume, the rate of evaporation is approximated during the time from the initial boiling point to the time of first drop recovered in the receiving cylinder as being equal to the rate of recovery between the first drop recovery point and the 5-mL recovery point from the D86 distillation.

$$V_{evap}(t) = V_{rec}(t) + V_{loss} + \frac{V_{FD-5\%}}{t^{D86}_{FD-5\%}} t_{IBP-FD} \tag{4}$$

In Eq. (4), $V_{FD-5\%}$ is the volume from the first drop to 5 mL recovered (i.e., $V_{FD-5\%}$ = 5 mL), $t^{D86}_{FD-5\%}$ is the time between the first drop recovered and 5-mL recovered volume for the D86 distillation, and t_{IBP-FD} is the time between the true initial boiling point and the first drop of condensate recovered in the receiving cylinder.

The approximation that the dynamic holdup remains constant during the distillation is based on the fact that recovery rate in the receiving cylinder is relatively steady throughout the distillation, as the heat flux applied to the distillation flask is continually adjusted to maintain a steady flow of condensate out of the condenser tube. An example of this steady recovery rate is shown in Fig. 6 for Mixture 1. During portions of the distillation where the temperature is approximately constant, such as from 70 to 90 vol

Table 2
IBP identified by second derivative minimum compared to IBP determined from the calculated equilibrium curve. T_{IBP}^{CE} is the initial boiling point determined from the calculated equilibrium curve, T_{IBP}^{2nd} is the initial boiling point determined from the minimum of the second derivative of the time-resolved data, $|\Delta T_{IBP}|$ (shown in bold font in the table) is the absolute difference between T_{IBP}^{CE} and T_{IBP}^{2nd}, t_{IBP}^{CE} is the time corresponding to the location of T_{IBP}^{CE} in the time-resolved data, t_{IBP}^{2nd} is the time corresponding to the location of the minimum of the second derivative from the data, and $|\Delta t_{IBP}|$ (shown in bold font in the table) is the absolute difference between t_{IBP}^{CE} and t_{IBP}^{2nd}.

Mixture	Run #	T_{IBP}^{CE} [°C]	T_{IBP}^{2nd} [°C]	$\|\Delta T_{IBP}\|$ [°C]	t_{IBP}^{CE} [s]	t_{IBP}^{2nd} [s]	$\|\Delta t_{IBP}\|$ [s]
1	1	198.4	200.2	**1.8**	591.0	606.7	**15.7**
	2	198.4	199.9	**1.5**	582.7	594.7	**12.0**
	3	198.4	200.2	**1.8**	579.8	594.8	**15.0**
	4	198.4	199.8	**1.4**	605.2	617.9	**12.7**
	5	198.4	199.7	**1.3**	591.4	601.7	**10.3**
2	1	54.3	54.5	**0.2**	493.6	496.0	**2.4**
	2	54.3	55.1	**0.8**	502.8	515.7	**12.9**
	3	54.3	54.8	**0.5**	539.5	547.3	**7.8**
3	1	71.2	71.4	**0.2**	384.7	394.2	**9.5**
	2	71.2	71.0	**0.2**	476.0	472.2	**3.8**
	3	71.2	70.6	**0.6**	435.8	417.2	**18.6**
4	1	48.6	50.7	**2.1**	422.2	439.2	**17.0**
	2	48.6	49.9	**1.3**	375.6	385.3	**9.7**

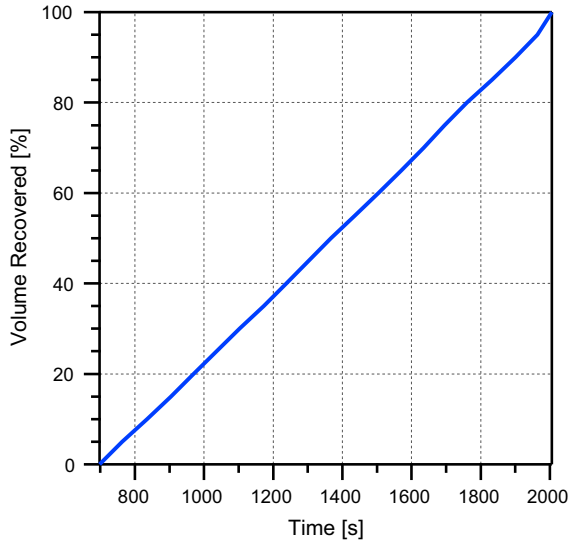

Fig. 6. Volume recovered in receiving cylinder versus time for a D86 distillation of Mixture 1 (50/50 n-decane/n-tetradecane).

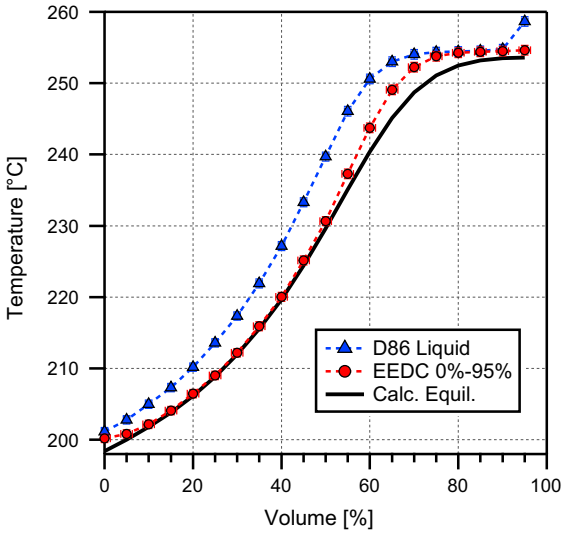

Fig. 7. Experimental equilibrium distillation curve (EEDC) plotted for 0–95 vol% compared to the original D86 liquid temperature distillation curve and calculated equilibrium distillation curve for Run 1 of Mixture 1 (50/50 n-decane/n-tetradecane). Error bars for liquid volume and temperature uncertainty are smaller than markers (±0.5 mL, ±0.8 °C). Error bars for EEDC uncertainty are almost exactly represented by marker size (±1.4 mL, ±0.8 °C).

% for Mixture 1 (see Fig. 1), the heat applied is also constant, which would be the case for a steadily evaporating mixture of constant composition. Fig. 6 shows that the volume recovered versus time is almost a perfectly straight line, indicating a steady recovery rate as well during the 70–90% recovery period. Therefore, no significant change in mass storage occurs during this period. This is assumed to also be the case for the rest of the distillation process after the transient period around the initial boiling point. It should be noted that when drastic changes in heat flux occur, such as near the end point of a distillation, this assumption may no longer be valid. For certain mixtures containing components with drastically different initial boiling points, this assumption may also be invalid.

The volume evaporated versus time is calculated according to Eq. (4). The volume evaporated curve is then interpolated to determine the times corresponding to 5-mL evaporated liquid increments for volumes from 5 mL to 95 mL. The time for 0 mL was determined from the IBP identification procedure described in Section 3.3.1. These times are used to identify the corresponding liquid temperature at each 5-mL evaporated interval, allowing liquid temperature versus volume evaporated plots to be constructed.

A representative n-decane/n-tetradecane distillation curve calculated using the described method, from 0% evaporated to 95% evaporated, is plotted in Fig. 7 and compared to the original D86 liquid temperature distillation curve and the calculated equilibrium distillation curve. Correcting the liquid temperature curve for dynamic holdup and any loss effectively shifts the liquid temperature distillation curve (measured at the D86 volume intervals). The new 0–95% evaporated distillation curve, now unaffected by dynamic holdup and losses, is clearly a much better approximation of an equilibrium curve than the D86 liquid temperature curve.

3.3.3. EP identification

Due to the drastic changes in heating rate and evaporation rate that occur as a distillation nears its end, the calculated 100 vol% point was not selected as the equilibrium curve end point. Instead, the final point of each experimental equilibrium curve is approximated as the vapor temperature (without emergent stem

Table 3
ASTM D86 end point vapor temperatures (no emergent stem error emulation applied) recorded for the four fuel mixtures of interest.

	Run #	ASTM D86 end point [°C]
Mixture 1	1	254.6
	2	254.4
	3	254.2
	4	254.6
	5	254.5
Mixture 2	1	98.6
	2	98.6
	3	98.0
Mixture 3	1	101.4
	2	101.2
Mixture 4	1	206.9
	2	207.9

error emulation applied) at the end point identified in accordance with the ASTM D86 standard procedure. The D86 end point is defined as the point when the vapor temperature measured in the flask neck reaches a maximum value [4]. This occurs when vapor fills the flask bulb and then rises to engulf the vapor RTD.

This point was chosen for two reasons. First, it has repeatedly been observed that the temperature within the distillation flask reaches a somewhat uniform value at the end of each distillation. Therefore, although this point corresponds to a temperature measured in the neck of the flask, it is assumed to reasonably approximate the temperature of the remaining saturated liquid at the bottom of the flask. Second, this point has physical significance in the distillation process. The end point indicates the temperature of the vapor when mass transfer past the RTD begins to drop significantly. This point is a feasible indicator of the temperature at which the transition from saturated liquid to saturated vapor reaches completion. The D86 end point vapor temperatures (with no emergent stem error emulation applied) recorded for multiple distillation runs for each of the four fuel mixtures of interest are listed in Table 3.

It should be noted that there is a relatively larger degree of uncertainty associated with the end point identified by D86 than the other points in the distillation. The end point temperatures are somewhat dependent on the heat flux applied to the flask at the end of each distillation. For a single fuel sample, the end points recorded for different distillation runs have been seen to differ by as much as 14 °C. However, when identical heating profiles are used, more repeatable results are observed, as seen in Table 3. The fact that the end point temperature is sensitive to the applied heat flux indicates that after the final heat adjustment is made, the temperature data is not solely indicative of the true boiling point of the remaining fuel mixture, but instead contains artifacts due to the experimental setup and procedure. These points are likely impacted by radiation from the electric heater in the apparatus, which may cause the temperature of the RTD probe to rise.

Further work in this area is needed. It is likely that D86-adherent distillation apparatuses are simply not well suited for accurately measuring the true final boiling point of a fuel without further modifications.

4. Results and discussion

4.1. Experimental equilibrium distillation curve (EEDC) results

The experimental equilibrium distillation curves (EEDCs) have been determined for the four mixtures in Table 1. For each mixture, data from the runs shown in Table 2 were used to determine an average EEDC (see Table 2 or Table 3 for the number of runs per mixture). Each mixture's average EEDC is plotted in Fig. 8, alongside its D86 average liquid temperature curve, its average D86 vapor curve, and its calculated equilibrium curve. The D86 liquid and vapor curves shown are corrected to standard atmospheric pressure using the Sydney Young equation. Each EEDC is therefore also reported at standard atmospheric pressure. As per ASTM D86, the D86 vapor curves also have emergent stem error emulation applied.

The error bars in Fig. 8 are calculated using the square root of the sum of the squared uncertainties. The temperature-axis uncertainties include the run-to-run repeatability and the errors associated with the RTD temperature measurements and correction using the Sydney Young equation. Run-to-run uncertainty is calculated at 95% confidence using a Student's *t*-distribution to estimate the standard deviation. The volume uncertainty for the D86 liquid and vapor curves includes 0.5-mL uncertainty due to the volume recovered and losses, and an estimated uncertainty of 0.1 mL corresponding to the residue measurement. The EEDC volume uncertainty includes the uncertainties associated with the D86 curves, as well as the impact of initial boiling point time uncertainty (estimated to be ±10 s) and the impact of the 0–5 vol % recovery time uncertainty (estimated to be ±5 s). These are included based on error analysis of Eq. (4).

The experimental equilibrium distillation curves seen in Fig. 8 show clear improvement over the liquid and vapor temperature curves in their ability to closely approximate the calculated equilibrium curve. The improvement of the EEDC relative to the standard ASTM D86 vapor measurement is quite significant. To demonstrate this more quantitatively, several key measures are tabulated in Tables 4–6, which give the mean absolute temperature difference, the maximum absolute temperature difference, and the difference in initial boiling point temperature between the three measured curves (D86 vapor, D86 liquid, and EEDC) and the calculated equilibrium distillation curve.

The mean absolute temperature difference for the experimental curves relative to the equilibrium curves is given in Table 4. The results illustrate a statistically significant improvement in the average difference for the EEDC curves relative to the D86 vapor and D86 liquid measurements. In particular, for fuels with high initial boiling points or wide boiling range fuels (Mixtures 1 and 4), the average difference drops substantially for the EEDC relative to the standard D86 vapor measurement. The EEDCs are within 2.2 °C of the calculated equilibrium curves.

The maximum absolute temperature difference, given in Table 5, is also lower for the EEDCs than for the D86 liquid and vapor curves. The improvement is very large for certain cases, such as Mixture 1, where the maximum difference occurs at the IBP and the maximum difference is reduced from 33 °C for the D86 vapor to 3 °C for the EEDC. One exception to this is observed for Mixture 3, which has a very steep increase in temperature around 30 vol%. This steep slope makes the temperature at a given volume % very sensitive to the volume measurement. With the added complication of only having three distillation runs to average for this case, large error bars for the EEDC result. As suggested by the lower average temperature difference for the Mixture 3 EEDC, only one point on the entire distillation curve is in worse agreement with the calculated equilibrium curve for the EEDC than for the D86 vapor curve; this point happens to correspond to the maximum temperature difference point for both curves (located at 30 vol%). It should be noted as well that due to the large uncertainty in the EEDC and vapor curves at this point, no statistically significant difference between the two is present.

Accurate determination of the IBP is essential, since the IBP significantly influences the vapor pressure of the fuel mixture. Table 6 shows the large improvement in initial boiling point determination for the EEDCs. The EEDCs identify the IBP within

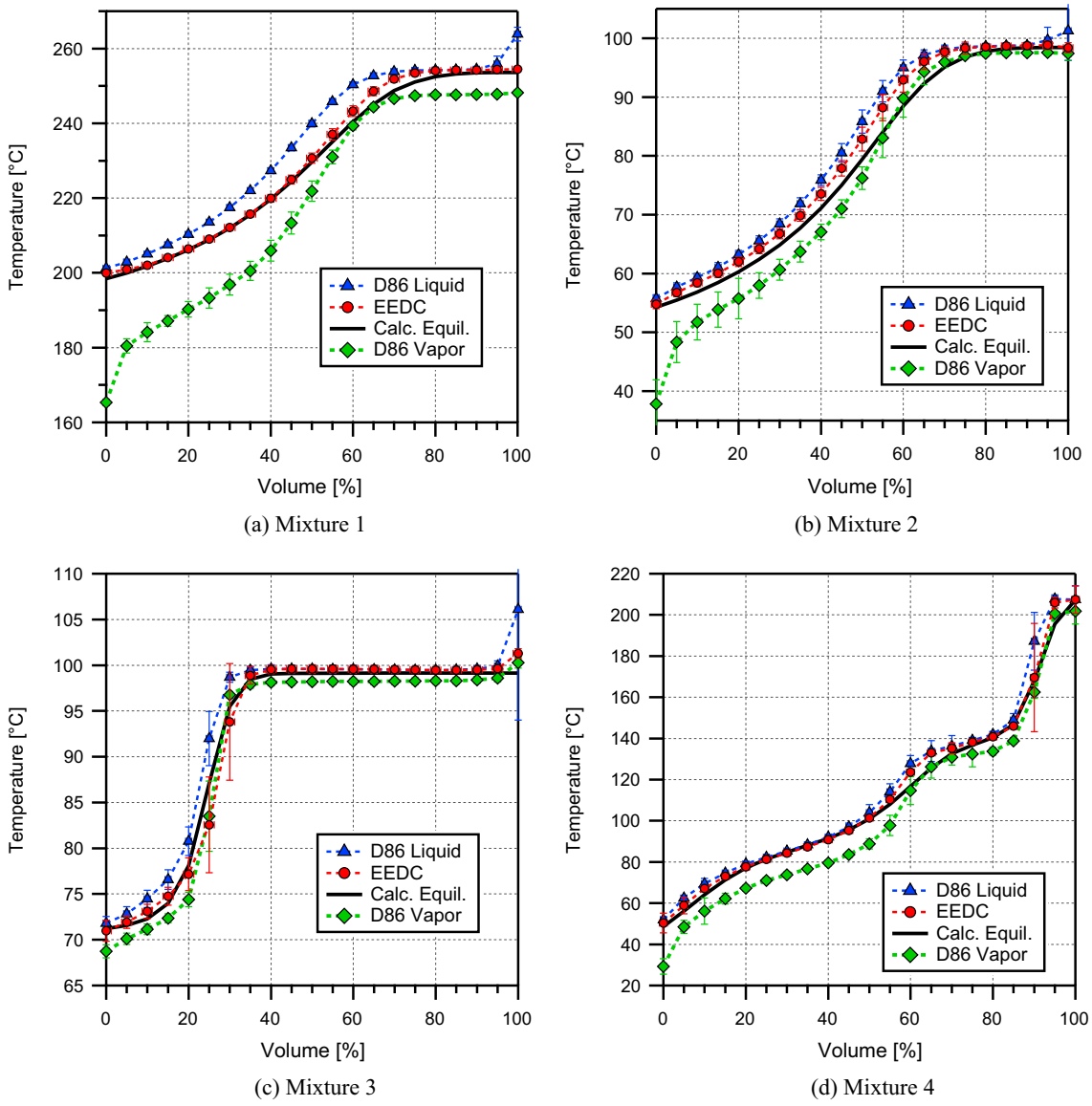

Fig. 8. Average experimental equilibrium distillation curves plotted alongside the average D86 liquid temperature measurement, the average D86 vapor temperature measurement, and the calculated equilibrium curve for: (a) Mixture 1 (50/50 n-decane/n-tetradecane), (b) Mixture 2 (50/50 n-heptane/n-pentane), (c) Mixture 3 (iso-octane, n-heptane, and ethanol), and (d) Mixture 4 (1-butene, 1-hexene, methyl pentanoate, and ethyl levulinate). Error bars for the equilibrium distillation curves (±2.45 K at 95% confidence) are not shown on the plots for clarity of presentation.

Table 4
Mean absolute temperature differences [°C] between the D86 vapor, D86 liquid, and EEDC measurements and the calculated equilibrium curve for the four mixtures. Uncertainties given correspond to 95% confidence level.

Mixture #	D86 vapor	D86 liquid	EEDC
1	10.5 ± 1.0	5.4 ± 0.3	1.2 ± 0.3
2	3.4 ± 1.4	3.2 ± 1.0	2.1 ± 0.8
3	1.3 ± 0.1	1.5 ± 1.0	0.8 ± 0.5
4	8.2 ± 2.2	4.5 ± 0.5	2.2 ± 1.4

Table 5
Maximum absolute temperature differences [°C] between the D86 vapor, D86 liquid, and EEDC measurements and the calculated equilibrium curve for the four mixtures. Uncertainties given correspond to 95% confidence level.

Mixture #	D86 vapor	D86 liquid	EEDC
1	33 ± 0.8	11 ± 1	3 ± 1
2	16 ± 4	7 ± 2	5 ± 2
3	4 ± 1	7 ± 12	5 ± 5
4	19 ± 4	19 ± 14	10 ± 3

2 °C of the calculated equilibrium value. These results are in direct contrast to the routinely used D86 vapor method, which yields IBP measurements that are off by as much as 33 °C (Mixture 1). The D86 vapor measurements only reasonably accurately determine the IBP for one case (Mixture 3); for the other three mixtures the IBP is off by more than 16 °C. The liquid temperatures reported at the D86 recovery points do a better job of estimating the IBP, but are still not as accurate as the EEDC results.

Overall, the EEDCs show good agreement with the calculated equilibrium curves. The liquid temperatures recorded at the D86 recovery points show improvement relative to the standard D86 vapor method (except at the distillation end point). However, the EEDC results have superior overall agreement with the calculated equilibrium curves.

Despite differences in ambient conditions and application of heat, each individual run's resulting EEDC closely resembles that

Table 6
Temperature differences [°C] between the initial boiling point (0 vol%) for the D86 vapor, D86 liquid, and EEDC measurements and the calculated equilibrium curve initial boiling point for the four mixtures. Uncertainties given correspond to 95% confidence level. A negative value indicates an IBP temperature that is lower than the calculated equilibrium IBP temperature.

Mixture #	D86 vapor	D86 liquid	EEDC
1	−33 ± 0.8	2.8 ± 0.6	1.6 ± 0.6
2	−16 ± 4	1.5 ± 0.7	0.5 ± 0.8
3	−2.5 ± 0.5	0.6 ± 0.8	−0.2 ± 1.2
4	−19 ± 4	3 ± 1	2 ± 5

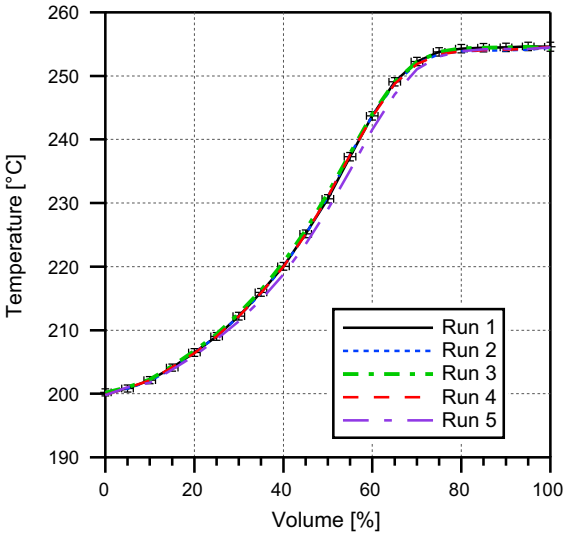

Fig. 9. Typical repeatability seen across five EEDCs for five separate distillation runs for Mixture 1 (50/50 n-decane/n-tetradecane mixture). For clarity, only error bars for run 1 are shown.

Table 7
Average dynamic holdup and difference between the IBP and the condenser bath temperature (in order of descending IBP).

Mixture	Average dynamic holdup [mL]	$T_{IBP} - T_{cond}$ [°C]
1	7.2 ± 0.7	176.4
3	4.1 ± 2.4	71.2
2	2.4 ± 0.9	54.3
4	1.4 ± 1.4	48.6

of the other runs for the same mixture, as evidenced by the generally small error bars for the EEDCs. Fig. 9 shows typical repeatability seen in individual run experimental equilibrium curves for the 50/50 n-decane/n-tetradecane mixture. The five EEDCs are essentially identical and within the error bounds associated with the RTD temperature measurement and EEDC volume determination.

4.2. Dynamic holdup magnitude

Dynamic holdup represents the majority of the shift in volume between the liquid D86 curves and the EEDCs. Because the evaporation rate and recovery rate are assumed to be equal after the transient period that occurs at the initial boiling point, the dynamic holdup is constant throughout the distillation process. The magnitude of the dynamic holdup, averaged over multiple distillation runs for each of the four fuel mixtures of interest, is shown in Table 7. Uncertainties indicate 95% confidence interval bounds for each value. Mixture 1 (50/50 n-decane/n-tetradecane) exhibits the largest dynamic holdup volume, while Mixture 4 (1-butene, 1-hexene, methyl pentanoate, and ethyl levulinate) exhibits the smallest dynamic holdup volume.

As the initial boiling point temperature of a fuel mixture increases, the dynamic holdup associated with the distillation of that mixture also tends to increase. Combined with the fact that dynamic holdup remains constant over the duration of a distillation, it can be inferred that dynamic holdup volume is largely impacted by the difference in the fuel's initial boiling point temperature and the condenser temperature, which is in turn dependent on a mixture's most volatile components. For complex mixtures it is anticipated that the composition profile, which influences the shape of the distillation curve, may also play a significant role in determining dynamic holdup. A comparison of the difference in initial boiling point and condenser temperature for the four fuel mixtures is included in Table 7.

For Mixtures 2, 3, and 4 explored in this work, a condenser bath temperature of 0–1 °C was used; for Mixture 1, an ambient-temperature (22 °C) condenser bath was used (in accordance with ASTM D86). For a higher initial boiling point with a fixed bath temperature, there is a larger temperature differential between the vapor initially entering the condenser and the condenser bath. As the difference between the initial vapor temperature and the condenser bath temperature increases, the dynamic holdup increases. A higher temperature differential will cause the vapor to condense earlier in the condenser tube; the larger temperature difference drives a higher rate of heat transfer from the vapor to the bath, leading to quicker condensation. As a result, a larger fraction of the condenser tube residence time is spent in liquid form. A lower temperature differential will result in the vapor condensing later in the condenser tube, meaning more of the tube will be traversed in the vapor phase.

The property actually controlling where in the condenser tube the first condensate is formed is the dew point of the most volatile components of the mixture. The dew point is related to the initial boiling point of the mixture, but depending on the mixture composition, the two parameters may not be directly correlated. For example, if a very volatile component makes up a small fraction of a low volatility mixture, then the initial boiling point is predominantly representative of the boiling points of the low volatility components. However, the most volatile components with low dew points are boiled off first and establish the dynamic holdup. This implies that dynamic holdup depends on the temperature and dimensions of the condenser tube and the mixture composition in a relatively complex fashion.

5. Application to petroleum distillate fuels

The developed experimental equilibrium distillation method was applied to investigate the differences between D86 distillation curves and equilibrium curves for cases where the precise fuel composition was not known. This was done for two fuels: an EPA EEE tier II certification gasoline (Haltermann Products) and a Naval F-76 #2 diesel fuel. Three distillations were performed for the EEE gasoline and four were performed for the F-76 diesel fuel. The results of the distillations are shown in Figs. 10 and 11 for the gasoline and diesel fuels, respectively.

Comparing the curves for the gasoline fuel, it is interesting to note that the liquid temperature closely approximates the EEDC except for the end point, which is too high. This close agreement is due to the small dynamic holdup for this mixture, which on average was found to be 0.7 ± 0.8 mL. Therefore, a good approximation to the EEDC would result from using the liquid D86 temperatures and then substituting the vapor D86 end point temperature (without emergent stem emulation applied) for the liquid D86 end point. The D86 vapor measurements are consistently lower than

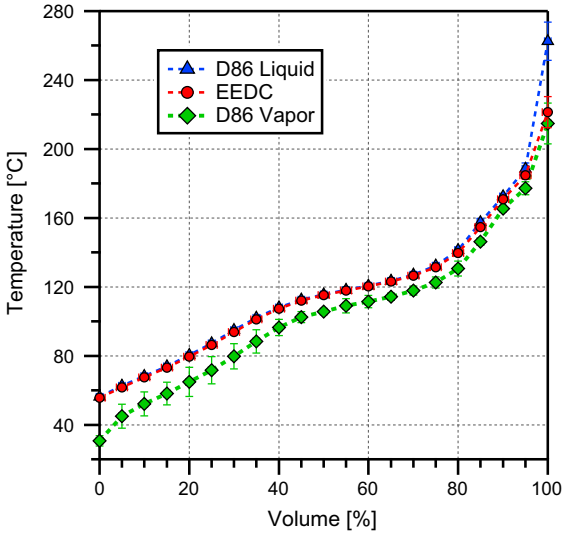

Fig. 10. Experimental equilibrium, D86 vapor, and D86 liquid distillation curves for a EEE tier II certification gasoline. Error bars represent 95% confidence level for temperature and volume. If error bars are not visible, they are smaller than the symbols.

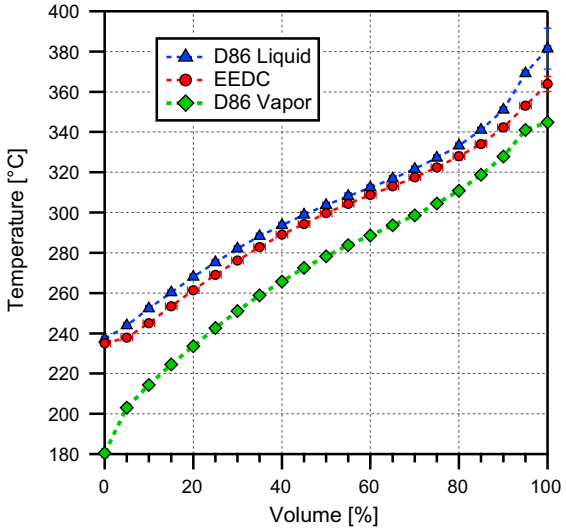

Fig. 11. Experimental equilibrium, D86 vapor, and D86 liquid distillation curves for an F-76 #2 diesel fuel. Error bars represent 95% confidence level for temperature and volume. If error bars are not visible, they are smaller than the symbols.

the EEDC, and underestimate the initial boiling point by 25 °C. This discrepancy will be very significant if the D86 curve is matched and used to estimate the Reid vapor pressure of the mixture. The resulting vapor pressure in this case would be much greater than that for the real fuel.

The F-76 diesel fuel results show significant differences between the EEDC and the D86 liquid and vapor measurements. The standard D86 vapor measurements show an incredibly large error in determination of the initial boiling point, with the D86 vapor IBP 55 °C lower than the EEDC identified IBP. The D86 vapor curve significantly underestimates the equilibrium curve temperature throughout the entire distillation. The liquid temperature is a much better approximation. However, the liquid temperature curve also shows measurable discrepancies and it overestimates the equilibrium temperatures. The greater discrepancy between the liquid curve and the EEDC for the diesel fuel is due to the larger dynamic holdup of 4.2 ± 0.7 mL for the diesel fuel.

6. Conclusion

Modifications were made to the D86 distillation measurement technique to allow for time-resolved vapor and liquid temperature and volume recovery measurements. A conceptual model was developed to describe the distillation process, thereby allowing a method to be derived that utilizes the time-resolved data to determine an experimental equilibrium distillation curve.

The method first identifies the IBP through analysis of the second derivative of liquid temperature with respect to time. A strong correspondence between the true IBP and the minimum of the 2nd derivative of temperature with respect to time was found, and the location of the local minimum in the 2nd derivative is taken as the time of the IBP. The volumetric evaporation rate between the newly identified IBP and the D86-identified IBP is approximated as the evaporation rate between the D86 IBP and the 5% recovery point. The volume recovery versus time for the D86 distillation measurements is adjusted using this initial evaporated volume estimate to give a volume evaporated versus time curve for the equilibrium distillation, assuming that the volume evaporated and volume recovered at any given time differ only by a constant (the sum of the dynamic holdup and evaporative loss) for the 5–95 vol% evaporated period. The time corresponding to each 5 vol% evaporated point is then used to find the corresponding liquid temperature at each volume point. Finally, the experimental end point of the D86 distillation (vapor temperature) is used as the end point (100% evaporated) for the distillation, as it represents the best estimate for the current setup. The result is an experimental equilibrium distillation curve, or EEDC.

The resulting experimental equilibrium distillation curves match the calculated equilibrium curves on average within a few degrees Celsius and represent a significant improvement in agreement compared with the traditional D86 distillation curve or a liquid temperature distillation curve that has not been shifted to account for dynamic holdup. For the four mixtures considered in this work, the EEDCs identify the IBP within 2 °C of the calculated equilibrium values. The maximum difference between an EEDC point and its corresponding equilibrium curve point is 10 ± 3 °C; for three of the four mixtures, the maximum difference between an EEDC point and its corresponding equilibrium curve point is 5 °C. The maximum mean absolute temperature difference between a final average EEDC and the corresponding equilibrium distillation curve for the four mixtures was found to be 2.2 ± 1.4 °C.

The dynamic holdup volume associated with the four fuel mixtures of interest was found to be between 1.4 and 7.2 mL. Dynamic holdup magnitude increases as the initial boiling point of a fuel increases and the temperature difference between the fuel sample and condenser bath increases. The dynamic holdup is also a complex function of the mixture composition.

Finally, the method was applied to investigate the difference between equilibrium curves and the ASTM D86 standard for two petroleum distillate fuels, a gasoline fuel and a diesel fuel, where the compositions were unknown. The results highlight the large errors relative to equilibrium curves if ASTM D86 results are used as approximations to equilibrium distillation curves.

Acknowledgement

This work was funded by the U.S. Department of Energy Great Lakes Bioenergy Research Center (DOE BER Office of Science DE-FC02-07ER64494).

References

[1] Pitz WJ, Cernansky NP, Dryer FL, Egolfopoulos FN, Farrell JT, Friend DG, et al. Development of an experimental database and chemical kinetic models for surrogate gasoline fuels. SAE technical paper series, 2007-01-0175; 2007.

[2] ASTM D4814: standard specification for automotive spark-ignition engine fuel, ed. West Conshohocken, PA: ASTM International; 2012.

[3] Alonso DM, Bond JQ, Dumesic JA. Catalytic conversion of biomass to biofuels. Green Chem 2010;12:1493–513.

[4] ASTM D86: standard test method for distillation of petroleum products at atmospheric pressure, vol. D86-10, ed. West Conshohocken, PA: ASTM International; 2010.

[5] Vapor pressure and vapor lock. J Franklin Inst, vol. 209; January 1930 [Notes from the U.S. Bureau of Standards].

[6] Motor Gasolines Technical Review, ed. San Ramon, CA: Chevron Corporation; 2004.

[7] Geng PY, Lund VA, Studzinski WM, Waypa TG, Belton DN. Gasoline distillation effect on vehicle cold start driveability. SAE technical paper series, 2007-01-4073; 2007.

[8] Greenfield ML, Lavoie GA, Smith CS, Curtis EW. Macroscopic model of the D86 fuel volatility procedure. SAE technical paper series, 982724; 1998.

[9] Spieksma W. Prediction of ASTM method D86 distillation of gasoline and naphthas according to the fugacity-filmmodel from gas chromatographic detailed hydrocarbon analysis. J Chromatogr Sci 1998;36.

[10] Bruno TJ. Improvements in the measurement of distillation curves. 1. A composition-explicit approach†. Ind Eng Chem Res 2006;45:4371–80.

[11] Bruno TJ. Method and apparatus for precision in-line sampling of distillate. Separ Sci Technol 2006;41:309–14.

[12] Ott LS, Smith BL, Bruno TJ. Experimental test of the Sydney Young equation for the presentation of distillation curves. J Chem Thermodyn 2008;40:1352–7.

[13] No. 103: Boiling Point. OECD Guidelines for the Testing of Chemicals, ed. The Organisation for Economic Co-operation and Development (OECD); 1995.

[14] Backhaus J. Design methodology of bio-derived gasoline fuels MS, Mechanical Engineering. Madison (WI): University of Wisconsin-Madison; 2013.

[15] Stichlmair JG, Fair JR. Distillation: principles and practices. Wiley; 1998.

[16] Hansen HK, Rasmussen P, Fredenslund A, Schiller M, Gmehling J. Vapor–liquid equilibria by UNIFAC group contribution. 5. Revision and extension. Ind Eng Chem Res 1991;30:2352–5. 2014/08/09.

[17] Yaws CL, Narasimhan PK, Gabbula C. Yaws' handbook of antoine coefficients for vapor pressure. 2nd electronic ed. Knovel; 2005.

[18] Ihmels EC, Gmehling J. Extension and revision of the group contribution method GCVOL for the prediction of pure compound liquid densities. Ind Eng Chem Res 2002;42:408–12. 2014/08/09.

[19] Poling BE, Prausnitz JM, O'Connell JP. Properties of gases and liquids. McGraw-Hill; 2000.

[20] Dimian A, Bildea C, Kiss A. Integrated design and simulation of chemical processes. Elsevier; 2014.